Physics Letters B 802 (2020) 135205

Contents lists available at ScienceDirect

Physics Letters B

www.elsevier.com/locate/physletb

Search for η mesic ^{3}He with the WASA-at-COSY facility in the $pd \to {}^3\mathrm{He}2\gamma$ and $pd \to {}^3\mathrm{He}6\gamma$ reactions

P. Adlarson [a], W. Augustyniak [b], W. Bardan [c], M. Bashkanov [d], S.D. Bass [c,e], M. Berłowski [f], A. Bondar [g,h], M. Büscher [i,j], H. Calén [a], I. Ciepał [k], H. Clement [l,m], E. Czerwiński [c], R. Engels [n], A. Erven [o], W. Erven [o], W. Eyrich [p], P. Fedorets [n,q], K. Föhl [r], K. Fransson [a], F. Goldenbaum [n], A. Goswami [n,s], K. Grigoryev [n,t], L. Heijkenskjöld [a,1], V. Hejny [n], S. Hirenzaki [u], L. Jarczyk [c], T. Johansson [a], B. Kamys [c], N.G. Kelkar [v], G. Kemmerling [o,2], A. Khreptak [c], D.A. Kirillov [w], S. Kistryn [c], H. Kleines [o,2], B. Kłos [x], W. Krzemień [y], P. Kulessa [k], A. Kupść [a,f], K. Lalwani [z], D. Lersch [n,3], B. Lorentz [n], A. Magiera [c], R. Maier [n,aa], P. Marciniewski [a], B. Mariański [b], H.-P. Morsch [b], P. Moskal [c], H. Ohm [n], W. Parol [k], E. Perez del Rio [l,m,4], N.M. Piskunov [w], D. Prasuhn [n], D. Pszczel [a,f], K. Pysz [k], J. Ritman [n,aa,ab], A. Roy [s], O. Rundel [c], S. Sawant [ac], S. Schadmand [n], I. Schätti–Ozerianska [c], T. Sefzick [n], V. Serdyuk [n], B. Shwartz [g,h], T. Skorodko [l,m,ad], M. Skurzok [c,*,4], J. Smyrski [c], V. Sopov [q], R. Stassen [n], J. Stepaniak [f], E. Stephan [x], G. Sterzenbach [n], H. Stockhorst [n], H. Ströher [n,aa], A. Szczurek [k], A. Trzciński [b,5], M. Wolke [a], A. Wrońska [c], P. Wüstner [o], A. Yamamoto [ae], J. Zabierowski [af], M.J. Zieliński [c], J. Złomańczuk [a], P. Żuprański [b], M. Żurek [n,6]

[a] Division of Nuclear Physics, Department of Physics and Astronomy, Uppsala University, Box 516, 75120 Uppsala, Sweden
[b] Department of Nuclear Physics, National Centre for Nuclear Research, ul. Pasteura 7, 02-093, Warsaw, Poland
[c] Institute of Physics, Jagiellonian University, prof. Stanisława Łojasiewicza 11, 30-348 Kraków, Poland
[d] School of Physics and Astronomy, University of Edinburgh, James Clerk Maxwell Building, Peter Guthrie Tait Road, Edinburgh EH9 3FD, United Kingdom of Great Britain and Northern Ireland
[e] Kitzbühel Centre for Physics, Kitzbühel, Austria
[f] High Energy Physics Department, National Centre for Nuclear Research, ul. Pasteura 7, 02-093, Warsaw, Poland
[g] Budker Institute of Nuclear Physics of SB RAS, 11 akademika Lavrentieva prospect, Novosibirsk, 630090, Russia
[h] Novosibirsk State University, 2 Pirogova Str., Novosibirsk, 630090, Russia
[i] Peter Grünberg Institut, PGI–6 Elektronische Eigenschaften, Forschungszentrum Jülich, 52425 Jülich, Germany
[j] Institut für Laser– und Plasmaphysik, Heinrich–Heine Universität Düsseldorf, Universitätsstr. 1, 40225 Düsseldorf, Germany
[k] The Henryk Niewodniczański Institute of Nuclear Physics, Polish Academy of Sciences, 152 Radzikowskiego St, 31-342 Kraków, Poland
[l] Physikalisches Institut, Eberhard–Karls–Universität Tübingen, Auf der Morgenstelle 14, 72076 Tübingen, Germany
[m] Kepler Center für Astro– und Teilchenphysik, Physikalisches Institut der Universität Tübingen, Auf der Morgenstelle 14, 72076 Tübingen, Germany
[n] Institut für Kernphysik, Forschungszentrum Jülich, 52425 Jülich, Germany
[o] Zentralinstitut für Engineering, Elektronik und Analytik, Forschungszentrum Jülich, 52425 Jülich, Germany
[p] Physikalisches Institut, Friedrich–Alexander–Universität Erlangen–Nürnberg, Erwin–Rommel-Str. 1, 91058 Erlangen, Germany
[q] Institute for Theoretical and Experimental Physics named by A.I. Alikhanov of National Research Centre "Kurchatov Institute", 25 Bolshaya Cheremushkinskaya, Moscow, 117218, Russia
[r] II. Physikalisches Institut, Justus–Liebig–Universität Gießen, Heinrich–Buff–Ring 16, 35392 Giessen, Germany
[s] Department of Physics, Indian Institute of Technology Indore, Khandwa Road, Simrol, Indore 453552, Madhya Pradesh, India
[t] High Energy Physics Division, Petersburg Nuclear Physics Institute named by B.P. Konstantinov of National Research Centre "Kurchatov Institute", 1 mkr. Orlova roshcha, Leningradskaya Oblast, Gatchina, 188300, Russia
[u] Department of Physics, Nara Women's University, Nara 630-8506, Japan

* Corresponding author.
E-mail address: magdalena.skurzok@uj.edu.pl (M. Skurzok).

[1] Present address: Institut für Kernphysik, Johannes Gutenberg–Universität Mainz, Johann–Joachim–Becher Weg 45, 55128 Mainz, Germany.
[2] Present address: Jülich Centre for Neutron Science JCNS, Forschungszentrum Jülich, 52425 Jülich, Germany.
[3] Present address: Department of Physics, Florida State University, 77 Chieftan Way, Tallahassee, FL 32306-4350, USA.
[4] Present address: INFN, Laboratori Nazionali di Frascati, Via E. Fermi, 40, 00044 Frascati (Roma), Italy.
[5] Deceased.
[6] Present address: Lawrence Berkeley National Laboratory, Berkeley, California 94720.

https://doi.org/10.1016/j.physletb.2020.135205

[v] Departamento de Fisica, Universidad de los Andes, Cra. 1E, 18A–10, Bogotá, Colombia
[w] Veksler and Baldin Laboratory of High Energiy Physics, Joint Institute for Nuclear Physics, 6 Joliot–Curie, Dubna, 141980, Russia
[x] August Chełkowski Institute of Physics, University of Silesia, Uniwersytecka 4, 40-007, Katowice, Poland
[y] High Energy Physics Division, National Centre for Nuclear Research, 05-400 Otwock-Świerk, Poland
[z] Department of Physics, Malaviya National Institute of Technology Jaipur, JLN Marg Jaipur 302017, Rajasthan, India
[aa] JARA–FAME, Jülich Aachen Research Alliance, Forschungszentrum Jülich, 52425 Jülich, and RWTH Aachen, 52056 Aachen, Germany
[ab] Institut für Experimentalphysik I, Ruhr–Universität Bochum, Universitätsstr. 150, 44780 Bochum, Germany
[ac] Department of Physics, Indian Institute of Technology Bombay, Powai, Mumbai 400076, Maharashtra, India
[ad] Department of Physics, Tomsk State University, 36 Lenina Avenue, Tomsk, 634050, Russia
[ae] High Energy Accelerator Research Organisation KEK, Tsukuba, Ibaraki 305–0801, Japan
[af] Department of Astrophysics, National Centre for Nuclear Research, 90–950 Łódź, Poland

ARTICLE INFO

Article history:
Received 25 September 2019
Received in revised form 7 January 2020
Accepted 7 January 2020
Available online 9 January 2020
Editor: L. Rolandi

Keywords:
η-mesic nuclei
η meson

ABSTRACT

We report on the experimental search for the bound state of an η meson and ^{3}He nucleus performed using the WASA-at-COSY detector setup. In order to search for the η-mesic nucleus decay, the $pd \to {}^3\mathrm{He}2\gamma$ and $pd \to {}^3\mathrm{He}6\gamma$ channels have been analysed. These reactions manifest the direct decay of the η meson bound in a ^{3}He nucleus. This non-mesonic decay channel has been considered for the first time. When taking into account only statistical errors, the obtained excitation functions reveal a slight indication for a possible bound state signal corresponding to a ^{3}He-η nucleus width Γ above 20 MeV and binding energy B_s between 0 and 15 MeV. However, the determined cross sections are consistent with zero in the range of the systematic uncertainty. Therefore, as final result we estimate only the upper limit for the cross section of the η-mesic ^{3}He nucleus formation followed by the η meson decay which varies between 2 nb and 15 nb depending on possible bound state parameters.

1. Introduction

Strong attractive interactions between the η meson and nucleons mean that there is a chance to form η meson bound states in nuclei [1]. If discovered in experiments, these mesic nuclei would be a new state of matter bound just by the strong interaction without electromagnetic Coulomb effects playing a role. Strong interaction bound states are formed in a different way as compared to exotic atoms which involve binding of electrically charged mesons with nuclei. For the latter, negatively charged pions or kaons could replace an electron in an outer orbital in a standard atom and get bound in the atom due to the Coulomb interaction. The charged meson in such an excited state quickly undergoes transitions to the lower states until it is close enough to the nucleus and is either absorbed by the nucleus or lost in a nuclear reaction. For strong interactions, in contrast to the pion, the neutral η meson is special due to the strong attractive nature of this meson-nucleon interaction [1]. An off-shell η meson produced in nuclear reactions such as the $pd \to {}^3\mathrm{He}2\gamma$ and $pd \to {}^3\mathrm{He}6\gamma$ below the η production threshold may form a bound state with the nucleus within which it is produced. Thus the absence of the electromagnetic interaction and the attractive nature of the η-nucleon interaction, makes the case of the neutral η meson different from that of the pion or the kaon and opens the possibility for an exotic nucleus made up of the meson and nucleons. Early experiments with low statistics using photon [2,3], pion [4], proton [5] or deuteron [6–9] beams gave hints for possible η mesic bound states but no clear signal [10,11].

Here we present a new high statistics search for ^{3}He-η bound states with data from the WASA-at-COSY experiment. We focus on the two main neutral decay channels of the η meson: $\eta \to 2\gamma$ with branching ratio $39.41 \pm 0.20\%$ and $\eta \to 3\pi^0 \to 6\gamma$ with branching ratio $31.54 \pm 0.22\%$ [12]. These processes constitute more than 70% of the η decays. The choice of neutral decay channels minimizes final state interactions involving charged particles. Concurrent measurement of the two channels increases the statistics and enables one to control systematic uncertainties in photons detection. The two-photon decay was previously suggested in [13] as a clean probe of the η in nuclear media.

Considering the η-nucleus interaction, bound states can be formed by the attractive interaction with finite level width corresponding to the finite lifetime of the state due to the absorptive interaction with the nucleus. The momentum distribution of the bound η meson determines the sum of the momenta of the emitted photons. Nuclear absorption and the additional η decay (disappearance) processes, reduces significantly the in-medium branching ratio of 2γ and 6γ decay channels [14].

η meson interactions with nucleons and nuclei are a topic of great experimental and theoretical interest. For recent reviews see [10,11,15–17]. Possible η-nucleus binding energies are related to the η-nucleon optical potential and to the value of η-nucleon scattering length $a_{\eta N}$ [18]. Phenomenological estimates for the real part of $a_{\eta N}$ are typically between 0.2 and 1 fm depending on the model assumptions. η bound states in helium require a large η-nucleon scattering length with real part greater than about 0.7–1.1 fm [19–21]. Recent calculations in the framework of optical potential [22], multi-body calculations [20], and pionless effective field theory [19] suggest a possible ^{3}He-η bound state.

Modifications of meson properties are expected in medium. In studies of the transparency of nuclei to propagating mesons produced in photoproduction experiments one finds strong η absorption in nuclei [24]. For the η' one finds weaker interaction with the nucleus. An effective mass shift for the η' in medium has been observed by the CBELSA/TAPS Collaboration [25]. The η'-nucleus optical potential $V_{\mathrm{opt}} = V_{\mathrm{real}} + iW$ deduced from these photoproduction experiments with a carbon target is $V_{\mathrm{real}}(\rho_0) = m^* - m = -37 \pm 10 \pm 10$ MeV and $W(\rho_0) = -10 \pm 2.5$ MeV at nuclear matter density ρ_0. This mass shift is very close to the prediction of the Quark Meson Coupling mode (QMC) with mixing angle -20 degrees [13,26], which also predicts a potential depth about -100 MeV for the η at ρ_0. The η' results are also consistent with scattering length estimates from COSY-11 [27] and Bonn [28]. Experimental

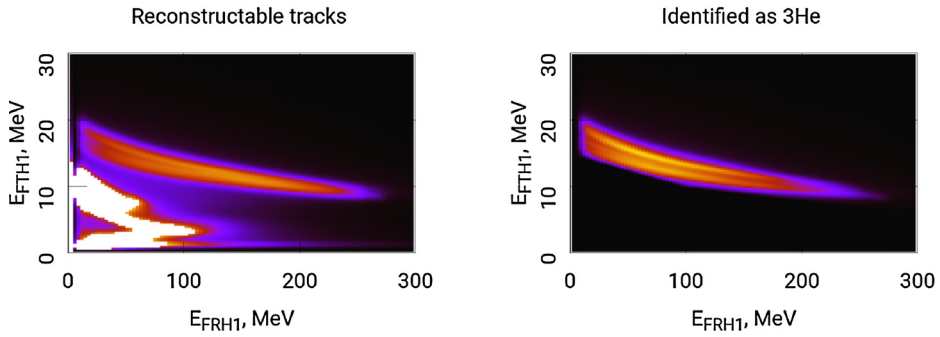

Fig. 1. 2-D histograms of energies deposited in the first layer of Forward Trigger Hodoscope (FTH1) and the first layer of Forward Range Hodoscope (FRH1) for all events with signal in Forward Proportional Chamber (FPC) (left panel) and events that were identified as ^{3}He (right panel).

search for η' - nucleus bound states has also been performed with results reported in Ref. [29].

Hints for possible η helium bound states are inferred from the observation of strong interaction in the η helium system. One finds a sharp rise in the cross section at threshold for η production in both photoproduction from ^{3}He [2,30] and in the proton-deuteron reaction $dp \rightarrow {}^3\mathrm{He}\eta$ [31]. These observations may hint at a reduced η effective mass in the nuclear medium.

Previous bound state searches at COSY have been focused on the reaction $dd \rightarrow {}^3\mathrm{He}N\pi$ [8,9]. Studies of the excitation function around the threshold for $dd \rightarrow {}^4\mathrm{He}\eta$ did not reveal a structure that could be interpreted as a narrow mesic nucleus. Upper limits for the total cross sections for bound state production and decay in the processes $dd \rightarrow ({}^4\mathrm{He}\text{-}\eta)_{bound} \rightarrow {}^3\mathrm{He}n\pi^0$ and $dd \rightarrow ({}^4\mathrm{He}\text{-}\eta)_{bound} \rightarrow {}^3\mathrm{He}p\pi^-$ were deduced to be about 5 nb and 10 nb for the $n\pi^0$ and $p\pi^-$ channels respectively [9]. The bound state production cross sections for $pd \rightarrow ({}^3\mathrm{He}\text{-}\eta)_{bound}$ [32] are expected to be more than 20 times larger than for $dd \rightarrow ({}^4\mathrm{He}\text{-}\eta)_{bound}$ [33].

In May 2014 the experiment searching for η mesic ^{3}He nuclei was performed at the COSY accelerator [34,35] in Jülich, Germany. The measurements were carried out using the WASA-at-COSY detector [36–40]. The mesic nuclei are supposed to be formed in proton-deuteron collisions. A ramped proton beam with beam momentum varying in the range from 1.426 to 1.635 GeV/c corresponding to ${}^3\mathrm{He}\eta$ excess energy range from −70 to 30 MeV and a pellet deuterium target [41] were used. The ^{3}He-η bound state was searched for in the $pd \rightarrow ({}^3\mathrm{He}\text{-}\eta)_{bound} \rightarrow {}^3\mathrm{He}2\gamma$ and $pd \rightarrow ({}^3\mathrm{He}\text{-}\eta)_{bound} \rightarrow {}^3\mathrm{He}6\gamma$ decay channels. These channels that manifest the direct decay of η bound in ^{3}He nucleus have been investigated for the first time. The existence of the bound ^{3}He-η state would manifest itself as a maximum or interference pattern in the excitation function for both of the studied reactions below the $pd \rightarrow {}^3\mathrm{He}\eta$ reaction threshold.

For the normalization of the excitation functions, the integrated luminosity was determined as a function of the excess energy. The analysis is presented in the next section. Further on, the data selection and efficiency determination is described. The data analysis is followed by the interpretation of the achieved excitation functions in view of the possible signal from the η-mesic ^{3}He.

2. Luminosity determination

Luminosity was determined based on the $pd \rightarrow {}^3\mathrm{He}\eta$ and $pd \rightarrow ppn_{spectator}$ reactions. The $pd \rightarrow {}^3\mathrm{He}\eta$ reaction analysis allows one to estimate the integrated luminosity for ${}^3\mathrm{He}\eta$ excess energy $Q_{{}^3He\eta}$ above zero. The ^{3}He particles were registered in the forward detector [36] and identified using the $\Delta E - E$ method based on energy losses in scintillator layers (see Fig. 1).

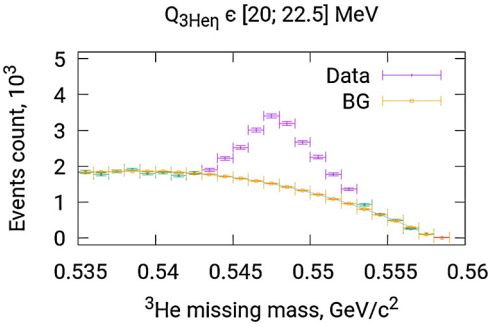

Fig. 2. ^{3}He missing mass spectrum obtained from data for the excess energy range of $Q_{{}^3He\eta} \in [20.0; 22.5]$ MeV. The part of the spectrum that is considered to be background is shown with green colour and is fitted with a polynomial of fourth power (orange).

The count of events originating from this reaction was obtained based on the ^{3}He missing mass spectra for each excess energy interval separately. An example spectrum is shown in Fig. 2. The reconstruction efficiency was calculated using Monte Carlo simulations taking into account the experimental data on cross sections and angular distributions [40,42–44].

The $pd \rightarrow ppn_{spectator}$ reaction analysis allows one to determine the integrated luminosity for the whole beam momentum range. As far as the target overlapping by the beam is changing during the acceleration cycle, the integrated luminosity value can change depending on the beam momentum. The registration efficiency for the $pd \rightarrow ppn_{spectator}$ reaction was obtained with dedicated Monte Carlo simulations described in Refs. [45,46]. The distribution of relative proton-neutron motion inside the target deuteron was calculated based on the parametrisation of the Paris potential [47]. Data on the proton-proton elastic scattering cross section and the angular distribution [48] were used for simulating the quasi-elastic scattering in the framework of the spectator model. The calculated cross section was multiplied by the factor 0.96 to take into account the shading effect [49]. It is worth noting that above the η production threshold, the two estimates of luminosity are in agreement (based on the $pd \rightarrow ppn_{spectator}$ and $pd \rightarrow {}^3\mathrm{He}\eta$ reactions [45]). The total integrated luminosity was determined to be $2446 \pm 3(stat.) \pm 66(syst.) \pm 4(\mathrm{norm.})$ nb^{-1} where the statistical, systematic and normalisation errors are indicated, respectively [45]. This is the largest statistics ever obtained for these experimental conditions.

3. The analysis of $pd \rightarrow ({}^3\mathrm{He}\text{-}\eta)_{bound} \rightarrow {}^3\mathrm{He}2\gamma$ and $pd \rightarrow ({}^3\mathrm{He}\text{-}\eta)_{bound} \rightarrow {}^3\mathrm{He}6\gamma$ reactions

As a first step, in order to establish the optimal selection criteria, Monte Carlo simulations for the $pd \rightarrow ({}^3\mathrm{He}\text{-}\eta)_{bound} \rightarrow {}^3\mathrm{He}2\gamma$

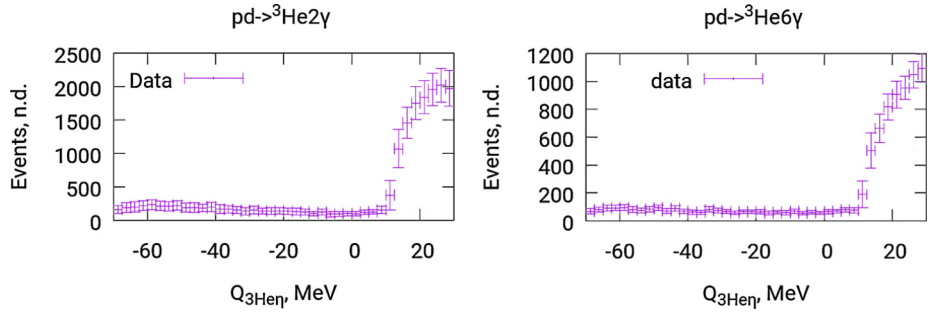

Fig. 3. The dependence of determined events count on $Q_{^3He\eta}$ for $pd \to {}^3\mathrm{He}2\gamma$ reaction (left panel) and $pd \to {}^3\mathrm{He}6\gamma$ reaction (right panel). The error bars include both statistical and systematic uncertainties.

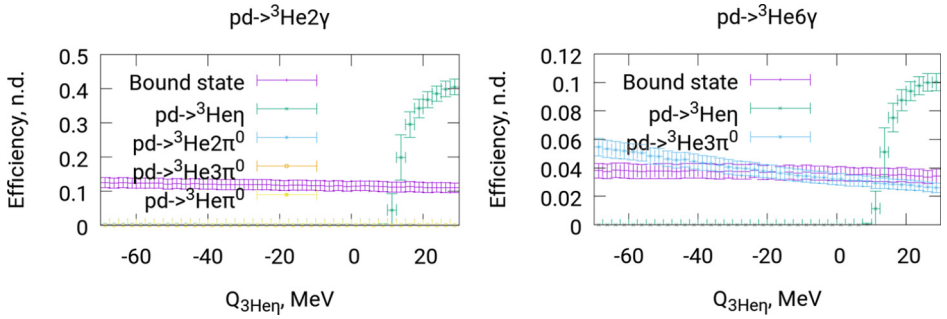

Fig. 4. The efficiency for different reactions when applying selection criteria defined for the $pd \to {}^3\mathrm{He}2\gamma$ (left) and $pd \to {}^3\mathrm{He}6\gamma$ (right) reaction analysis.

and $pd \to ({}^3\mathrm{He}\text{-}\eta)_{bound} \to {}^3\mathrm{He}6\gamma$ reactions were performed in the framework of the spectator model with the assumption of an isotropic distribution of bound η meson decay products in its rest frame. The momentum of the η meson was simulated using the recent model [14] in which the ^{3}He-η relative momentum distribution was calculated by solving the Klein-Gordon equation assuming the potential of η-nucleus interaction based on Hiyama's density distribution in ^{3}He [50–52].

For the $pd \to ({}^3\mathrm{He}\text{-}\eta)_{bound} \to {}^3\mathrm{He}2\gamma$ reaction analysis, the events containing a ^{3}He track in the forward detector and at least two photons in the central detector were selected. If there were more than two photons, the pair with the invariant mass closest to the η mass corrected by $Q_{^3He\eta}$ value was chosen. Then the restrictions on ^{3}He missing mass, γ-γ missing mass, and γ-γ invariant mass were applied using selection ranges based on the simulated distributions [45]. The excitation function obtained for the $pd \to {}^3\mathrm{He}2\gamma$ reaction is shown in the left panel of Fig. 3.

The signal from the bound state is expected for excess energies around or below zero. The increase of events above 10 MeV is due to the $pd \to {}^3\mathrm{He}\eta$ reaction. It starts at 10 MeV because of a hole for the COSY beam in the geometrical acceptance of the WASA-at-COSY detector (see Fig. 4).

For the $pd \to ({}^3\mathrm{He}\text{-}\eta)_{bound} \to {}^3\mathrm{He}6\gamma$ reaction analysis, the events containing a ^{3}He track in the forward detector and at least six photons in the central detector were selected. For each combination forming three pairs, to identify the $\eta \to 3\pi^0 \to 6\gamma$ decay, the following quantity is calculated:

$$D = \sum_{i=1}^{3} (m_{\gamma_{(2i-1)}\gamma_{2i}} - m_{\pi^0})^2 \qquad (1)$$

where $m_{\gamma_{(2i-1)}\gamma_{2i}}$ is the γ pair invariant mass and m_{π^0} is π^0 mass. The combination of six photons that minimises D was chosen. Then analogous to the 2γ case, the selection conditions on the ^{3}He missing mass, 6γ invariant mass, and 6γ missing mass were applied based on the simulated distributions [45]. The excitation function obtained for the $pd \to {}^3\mathrm{He}6\gamma$ reaction is shown in the right panel of Fig. 3.

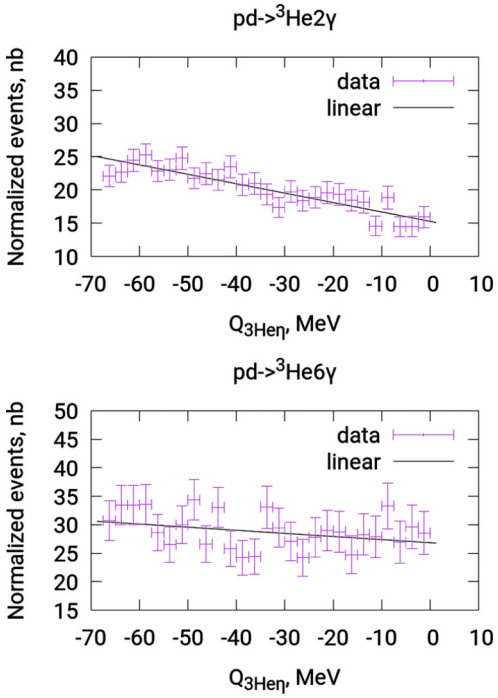

Fig. 5. Excitation curves determined for the $pd \to ({}^3\mathrm{He}\text{-}\eta)_{bound} \to {}^3\mathrm{He}2\gamma$ (upper panel) and $pd \to ({}^3\mathrm{He}\text{-}\eta)_{bound} \to {}^3\mathrm{He}6\gamma$ (lower panel) reactions. Superimposed lines indicate result of the fit of the line. The points above the η production threshold are excluded from the analysis.

The excitation curves have been normalised using the integrated luminosity values calculated based on the $pd \to ppn_{spectator}$ reaction and the efficiency determined based on Monte Carlo simulations. The results for both studied reactions are shown in Fig. 5.

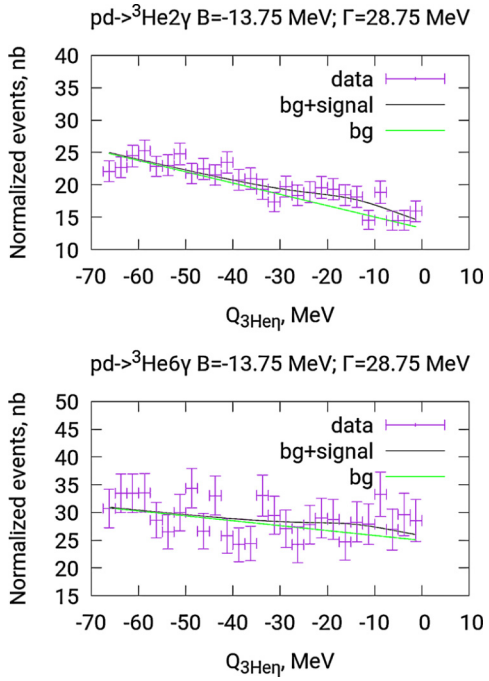

Fig. 6. Exemplary result of the simultaneous fit of functions (2) and (3) to the experimental data for the assumed B_s and Γ values as indicated above the figures. Superimposed black line shows the full fit result, and the green line shows the background function only.

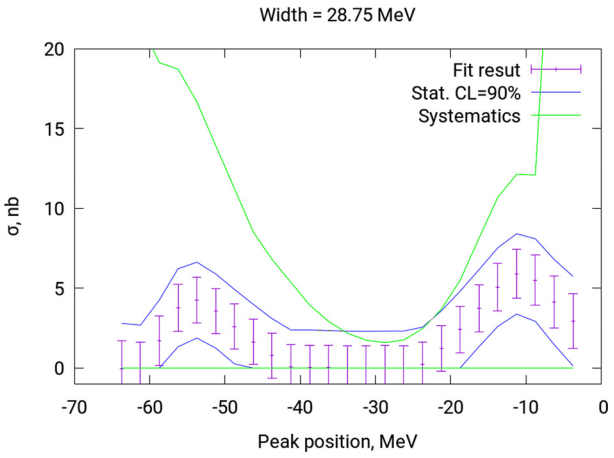

Fig. 7. Upper limits for the bound state production cross section via $pd \to (^3\text{He-}\eta)_{bound} \to {}^3\text{He}(\eta$ decays) as function of binding energy for fixed width Γ=28.75 MeV. The values of the Breit-Wigner amplitude σ are shown with statistical uncertainties. The range of possible bound state production cross section obtained based on statistical uncertainty corresponding to 90% confidence level is shown by blue lines. The range of possible bound state production cross section including systematic uncertainty is shown by green lines.

4. The upper limit for the η mesic ^{3}He production cross section

The excitation curves obtained in the analysis (Fig. 5) did not reveal any resonance-like structures and the fit with linear functions results in χ^2 value < 1 when normalized to the number of degrees of freedom. This indicates that no strong signal from the bound ^{3}He-η state is observed.

Further on, for the quantitative estimates of the upper limits for the bound state production, a fit to the excitation curves with a linear function (for background) plus a Breit-Wigner function (for the signal) was performed. The fit was done for different combinations of the assumed η-mesic ^{3}He binding energies B_s and widths Γ. The value of Γ was tested in the range from 1.25 MeV to 38.75 MeV (with the step of 2.5 MeV) and B_s in the range from 1.25 MeV to 63.75 MeV (with the step of 2.5 MeV).

For a given B_s and Γ pair, the following functions were fit simultaneously for the two studied reaction channels:

$$\rho^{fit}_{^3\text{He}2\gamma}(Q_{^3\text{He}\eta}) = P_{\eta\to 2\gamma}\cdot\sigma\cdot\sigma_b(Q_{^3\text{He}\eta}) + p_1 Q_{^3\text{He}\eta} + p_2, \quad (2)$$

$$\rho^{fit}_{^3\text{He}6\gamma}(Q_{^3\text{He}\eta}) = P_{\eta\to 6\gamma}\cdot\sigma\cdot\sigma_b(Q_{^3\text{He}\eta}) + p_3 Q_{^3\text{He}\eta} + p_4. \quad (3)$$

Here σ, p_1, p_2, p_3, and p_4 are the free fit parameters, $P_{\eta\to 2\gamma}$ and $P_{\eta\to 6\gamma}$ are the branching ratios for the $\eta\to 2\gamma$ and $\eta\to 6\gamma$ decays. Assuming that the ratio of branching ratios for the $\eta\to 2\gamma$ and $\eta\to 3\pi^0$ decay channels for the bound η meson remain the same as in vacuum, the vacuum branching ratio values of $P_{\eta\to 2\gamma}$ = 0.3941 and $P_{\eta\to 3\pi^0\to 6\gamma}$ = 0.3268 were used for performing the fit [12]. The function $\sigma_b(Q_{^3He\eta})$ in the fit formulae represents a Breit-Wigner shape which for a given values of B_s and Γ reads:

$$\sigma_b(Q_{^3He\eta}, B_s, \Gamma) = \sigma\,\frac{\Gamma^2/4}{(Q_{^3He\eta} - B_s)^2 + \Gamma^2/4}. \quad (4)$$

Example results of the fit are shown in Fig. 6. The figure shows results for the B_s and Γ values (indicated above the plots) for which the fitted values of σ differ from zero with the largest statistical significance. Fig. 7 indicates the results of the fit as a function of the B_s for the most promising value of Γ = 28.75 MeV.

The upper limit of the total cross section was determined based on the fit parameter uncertainty $\Delta\sigma^{stat}$:

$$\sigma^{CL=90\%}_{upper}(B_s, \Gamma) = \sigma + k\Delta\sigma^{stat}, \quad (5)$$

where k is the statistical factor equal to 1.64 corresponding to 90% confidence level as given in PDG [12]). Fig. 7 shows the systematic limits (blue lines) in addition to the statistical uncertainties (green lines). Systematic errors were estimated by changing the parameters of all cuts applied in the data analysis, and changing the values of assumed potential parameters for the ^{3}He-η interaction that determines the Fermi momentum distribution for relative motion in the bound state. The highest contribution to the systematic error is connected with the background fit function. The uncertainty due to the fit of quadratic or linear function estimated as $\sigma_{quad} - \sigma_{lin}$ varies from about 2 to 5 nb.

In the obtained excitation functions one can see a slight signal from the possible bound state for $\Gamma > 20$ MeV and $B_s \in [0; 15]$ MeV corresponding to the optical potential parameters $-100 < V_0 < -70$ MeV and $|W_0| > 20$ MeV in the model described in [14]. The result is also consistent with the QMC prediction of a potential depth about -100 MeV at nuclear matter density [13] and with the models in Refs. [19,20,22,23]. The allowed V_0-W_0 area is however different to those deduced from the η-^{4}He system [54] using the optical model of Ikeno et al. [53] where most of the model parameter space was excluded allowing values of the real and imaginary parts of the potential only between zero and about -60 MeV and -7 MeV respectively. However, the observed signal is within the range of the systematic uncertainty. Hence one cannot make definite conclusions whether η-mesic ^{3}He exists with the decay mechanism studied here.

5. Conclusions

The analysis of the $pd \to {}^3\text{He}2\gamma$ and $pd \to {}^3\text{He}6\gamma$ reactions has been performed in order to search for the existence of an η-mesic ^{3}He state. The analysis of the obtained excitation functions for the $pd \to {}^3\text{He}2\gamma$ and $pd \to {}^3\text{He}6\gamma$ reactions shows slight indication of the signal from the bound state for $\Gamma > 20$ MeV and

$B_s \in [0; 15]$ MeV. However, the observed indication is within the range of the systematic error which does not allow one to make a definite conclusion on a possible bound state formation.

The upper limit for the cross section of the bound state production varies between 2 and 15 nb depending on the bound state parameters. It is however important to stress that the determined upper limit concerns the production of the $(^3\text{He}\text{-}\eta)_{bound}$ state and its subsequent disintegration via decay of the η meson. The branching ratio for the latter in the nuclear medium remains to be estimated theoretically.

This is the first result obtained for the direct decay of bound η meson. The upper limit is much lower than the limit of 70 nb for $pd \to (^3\text{He}\text{-}\eta)_{bound} \to {}^3\text{He}\pi^0$ reaction obtained by the COSY-11 Collaboration [55] and is comparable with the upper limits obtained for the $dd \to (^4\text{He}\text{-}\eta)_{bound} \to {}^3\text{He}n\pi^0$ and $dd \to (^4\text{He}\text{-}\eta)_{bound} \to {}^3\text{He}p\pi^-$ reactions [9]. The much improved constraint will help tuning theoretical modelling of the η-nucleon and η-nucleus interactions.

Acknowledgements

We acknowledge the support from the Polish National Science Center through grant No. 2016/23/B/ST2/00784, and from the Foundation for Polish Science through the MPD and TEAM POIR.04.04.00-00-4204/17 programmes. Theoretical parts of this work was partly supported by the Faculty of Science, Universidad de los Andes, Colombia, through project number P18.160322. 001-17, and by JSPS KAKENHI Grant Numbers JP16K05355 (S.H.) in Japan.

References

[1] Q. Haider, L.C. Liu, Phys. Lett. B 172 (1986) 257.
[2] F. Pheron, et al., Phys. Lett. B 709 (2012) 21.
[3] V.A. Baskov, et al., PoS Baldin-ISHEPP-XXI (2012) 102.
[4] R.E. Chrien, et al., Phys. Rev. Lett. 60 (1988) 2595.
[5] A. Budzanowski, et al., COSY-GEM Collaboration, Phys. Rev. C 79 (2009) 012201.
[6] S.V. Afanasiev, et al., Phys. Part. Nucl. Lett. 8 (2011) 1073.
[7] P. Moskal, J. Smyrski, Acta Phys. Pol. B 41 (2010) 2281.
[8] P. Adlarson, et al., Phys. Rev. C 88 (2013) 055208.
[9] P. Adlarson, et al., Nucl. Phys. A 959 (2017) 102.
[10] V. Metag, M. Nanova, E.Y. Paryev, Prog. Part. Nucl. Phys. 97 (2017) 199.
[11] N.G. Kelkar, K.P. Khemchandani, N.J. Upadhyay, B.K. Jain, Rep. Prog. Phys. 76 (2013) 066301.
[12] M. Tanabashi, et al., Particle Data Group, Phys. Rev. D 98 (2018) 030001.
[13] S.D. Bass, A.W. Thomas, Phys. Lett. B 634 (2006) 368.
[14] M. Skurzok, et al., Nucl. Phys. A 993 (2020) 121647.
[15] S.D. Bass, P. Moskal, Rev. Mod. Phys. 91 (2019) 015003.
[16] B. Krusche, C. Wilkin, Prog. Part. Nucl. Phys. 80 (2014) 43.
[17] C. Wilkin, Eur. Phys. J. A 53 (6) (2017) 114.
[18] T.E.O. Ericson, W. Weise, Int. Ser. Monogr. Phys. 74 (1988).
[19] N. Barnea, B. Bazak, E. Friedman, A. Gal, Phys. Lett. B 771 (2017) 297, Erratum: Phys. Lett. B 775 (2017) 364.
[20] N. Barnea, E. Friedman, A. Gal, Nucl. Phys. A 968 (2017) 35.
[21] A. Fix, O. Kolesnikov, Phys. Lett. B 772 (2017) 663.
[22] J.J. Xie, W.H. Liang, E. Oset, P. Moskal, M. Skurzok, C. Wilkin, Phys. Rev. C 95 (1) (2017) 015202.
[23] N.G. Kelkar, Phys. Rev. Lett. 99 (2007) 210403.
[24] M. Nanova, et al., CBELSA/TAPS Collaboration, Phys. Lett. B 710 (2012) 600.
[25] M. Nanova, et al., CBELSA/TAPS Collaboration, Phys. Lett. B 727 (2013) 417.
[26] S.D. Bass, A.W. Thomas, Acta Phys. Pol. B 45 (2014) 627.
[27] E. Czerwinski, et al., Phys. Rev. Lett. 113 (2014) 062004.
[28] A.V. Anisovich, et al., Phys. Lett. B 785 (2018) 626.
[29] Y.K. Tanaka, et al., Phys. Rev. Lett. 117 (2016) 202501.
[30] M. Pfeiffer, et al., Phys. Rev. Lett. 92 (2004) 252001.
[31] P. Adlarson, et al., WASA-at-COSY Collaboration, Phys. Lett. B 782 (2018) 297.
[32] C. Wilkin, Acta Phys. Pol. B 45 (3) (2014) 603.
[33] S. Wycech, W. Krzemien, Acta Phys. Pol. B 45 (3) (2014) 745.
[34] R. Maier, Nucl. Instrum. Methods A 390 (1997) 1.
[35] D. Prasuhn, et al., IKP Annual Report, 2006.
[36] H.-H. Adam, et al., arXiv:nucl-ex/0411038, 2004.
[37] C. Bargholtz, et al., Nucl. Instrum. Methods A 594 (2008) 339.
[38] P. Adlarson, et al., Phys. Lett. B 707 (2005) 243.
[39] P. Adlarson, et al., Phys. Rev. C 90 (2014) 045207.
[40] P. Adlarson, et al., Phys. Lett. B 782 (2018) 297.
[41] Chr Bargholtz, et al., Nucl. Instrum. Methods A 587 (2008) 178.
[42] T. Rausmann, et al., Phys. Rev. C 80 (2009) 017001.
[43] T. Mersmann, et al., Phys. Rev. Lett. 98 (2007) 242301.
[44] R. Bilger, et al., Phys. Rev. C 65 (2002) 044608.
[45] O. Rundel, Doctoral Thesis, Jagiellonian University, 2019, arXiv:1905.04544.
[46] P. Moskal, R. Czyzykiewicz, AIP Conf. Proc. 950 (2007) 118.
[47] M. Lacombe, et al., Phys. Lett. B 101 (1981) 139.
[48] SAID database: http://www.gwu.edu/, The CNS Data Analysis Center.
[49] E. Chiavassa, et al., Phys. Lett. B 337 (1994) 192.
[50] E. Hiyama, Y. Kino, M. Kamimura, Prog. Part. Nucl. Phys. 51 (2003) 223.
[51] E. Hiyama, B.F. Gibson, M. Kamimura, Phys. Rev. C 70 (2004) 031001.
[52] E. Hiyama, Private communication.
[53] N. Ikeno, H. Nagahiro, D. Jido, S. Hirenzaki, Eur. Phys. J. A 53 (2017) 194.
[54] M. Skurzok, P. Moskal, N.G. Kelkar, S. Hirenzaki, H. Nagahiro, N. Ikeno, Phys. Lett. B 782 (2018) 6.
[55] W. Krzemien, et al., Acta Phys. Pol. Suppl. 2 (2009) 141.